Journal of ELECTRONIC MATERIALS, Vol. 39, No. 1, 2010
DOI: 10.1007/s11664-009-0951-8
© 2009 TMS

Growth of Intermetallic Compounds in Thermosonic Copper Wire Bonding on Aluminum Metallization

HUI XU,[1,3] CHANGQING LIU,[1] VADIM V. SILBERSCHMIDT,[1] and ZHONG CHEN[2]

1.—Wolfson School of Mechanical and Manufacturing Engineering, Loughborough University, Loughborough LE11 3TU, UK. 2.—School of Materials Science and Engineering, Nanyang Technological University, Nanyang Avenue, Singapore 639798, Singapore. 3.—e-mail: H.Xu3@lboro.ac.uk

Interface evolution caused by thermal aging under different temperatures and durations was investigated by means of scanning electron microscopy (SEM) and transmission electron microscopy (TEM). It was found that approximately 30-nm-thick and discontinuous Cu-Al intermetallic compounds (IMCs) were present in the initial bonds before aging. Cu-Al IMCs grew under thermal aging with increasing aging time. The growth kinetics of the Cu-Al IMCs was correlated to the diffusion process during aging; their combined activation energy was estimated to be 1.01 eV. Initially, Al-rich Cu-Al IMCs formed in the as-bonded state and early stage of aging treatment. Cu_9Al_4 was identified by selected-area electron diffraction (SAD) as the only type of Cu-Al IMC present after thermal aging at 250°C for 100 h; this is attributed to the relatively short supply of aluminum to the interfacial reaction.

Key words: Copper wire bonding, interfacial analysis, intermetallic compounds, growth kinetics, bonding mechanism

INTRODUCTION

Wire bonding is a key technique to provide electrical interconnections between integrated circuit (IC) chips and lead frames in microelectronics. The most commonly used process is thermosonic bonding of Au wire to Al metallization. However, this bonding system can easily lead to formation of Au-Al intermetallic compounds (IMCs).[1–6] Such IMCs are associated with Kirkendall voids, detrimentally affecting the reliability of components, especially in high-power devices and fine-pitch electronic applications. The use of Cu wire for thermosonic ball bonding presents several advantages over the use of Au wire, including significant cost saving, higher electrical and thermal conductivity for faster die functionality, and better mechanical properties.[7–9] Furthermore, because of the much slower IMC growth between the copper wire and aluminum metallization, Cu-Al bonds could potentially have a prolonged lifetime compared with Au-Al bonds.

Formation of IMCs and potential voids and cracks have a significant effect on the strength and reliability of bonds. A proper amount of IMCs formed in a wire bond increases the bonding strength, but their excessive growth can result in performance degradation of the bond. Increased growth of IMCs can also result in greater brittleness and contact resistance increase, leading to more heat generation in service. This, in turn, accelerates the growth of IMCs, finally causing failure of such bonds. In gold wire bonding, Au-Al IMCs have been observed at the interface in the as-bonded state, with a typical thickness of 200 nm to 500 nm.[10,11] Such initial Au-Al IMCs grow quickly during moulding and device operation due to thermally activated reactive diffusion, causing mechanical and electrical failure, known as "purple plague."[1] Compared with the rapid growth of Au-Al IMCs, the growth of Cu-Al IMCs was reported to be much slower.[12–14] Previous scanning electron microscopy (SEM) studies of Cu-Al bond interfaces found no Cu-Al IMCs in the

(Received March 10, 2009; accepted September 9, 2009; published online September 24, 2009)

bonds in the as-bonded state.[12,13] Studies by Kim et al. showed that the growth rate of Cu-Al IMCs between the copper and Al-1% Si-0.5% Cu metallization was approximately 1/10 of that for Au-Al IMCs in the temperature range of 150°C to 300°C.[14] The atomic properties of the elements (i.e., copper, gold, and aluminum) could be used to explain the large difference in the growth rates of IMCs. Compared with an atom of Au, an atom of Cu has a larger size misfit with aluminum and lower electronegativity, thus making the formation of Cu-Al IMCs much more difficult than the formation of Au-Al IMCs.[13] However, the kinetics of Cu-Al IMCs, including their activation energy, in thermosonic Cu-Al bonds was not clearly documented, although there were some studies on bulk and thin-film Cu-Al couples.[15–19]

Different IMCs can be formed at the interface and affect the reliability of bonds. IMCs with high melting points (e.g., above 1000°C) are stable at interfaces and should not significantly affect reliability. IMCs with low melting points (e.g., below 500°C) are less stable and their constituents will continue to diffuse, which can affect reliability. According to the binary phase diagram of the Cu-Al system, five IMCs—$CuAl_2$ (θ phase), CuAl (η_2 phase), Cu_4Al_3 (ζ_2 phase), Cu_3Al_2 (δ phase), and Cu_9Al_4 (γ_2 phase)—can exist at temperatures below 300°C.

Previously, studies of the interfacial behavior of Cu-Al bonds were mostly carried out using optical microscopy (OM) and SEM with an energy-dispersive x-ray spectrometer (EDX).[10–13] It should be noted that these techniques are not able to provide detailed information on crystallographic structure, therefore the expected intermetallic phases in Cu-Al bonds were not clearly identified. Transmission electron microscopy (TEM) is able to analyze the Cu-Al bond interface on the nanoscale and identify its crystallographic structure. The main challenge for TEM analysis of a wire bond is associated with specimen preparation since region-specific analysis is necessary. In addition, conventional specimen preparation can result in mechanical damage of the interface region during polishing. These problems can be overcome by using a dual-beam focused ion beam (FIB) system, which combines SEM with a scanning ion beam. In this way specific regions can be located using SEM, and TEM specimen prepared without the application of mechanical forces.

In this paper, we report the interfacial morphology of copper bonds on aluminum metallization in the as-bonded state, followed by the growth characteristics of Cu-Al IMCs at high temperatures and extended aging times. The growth kinetics of Cu-Al IMCs is examined as well as the effect of aging temperature and time on the morphology of IMCs. Finally, the intermetallic compounds in the bonds are identified by selected-area electron diffraction (SAD) on specimens prepared by a dual-beam FIB system. We also attempt to elucidate the mechanism of interfacial reaction between the copper wire and aluminum metallization during the bonding process and thermal aging.

EXPERIMENTAL PROCEDURES

In our experimental studies, a copper wire (99.99 wt.%) with a diameter of 50.8 μm was bonded to a 3-μm-thick Al metallization pad on a silicon chip using an ASM Eagle 60 ball/wedge automatic bonder with an ultrasonic frequency of 138 kHz. An electronic flame-off (EFO) process was applied to produce a spherical ball at the end of copper wire as the first step of the bonding cycle. The initial copper ball was achieved with a current of 150 mA and a gap voltage of 5500 V with a discharge time of 1.3 ms. In order to prevent the copper ball from oxidizing in the EFO process, a protective shielding gas—95% N_2 + 5% H_2—was supplied and maintained at a flow rate of 0.8 L/min. The copper ball was then bonded to aluminum metallization using a combination of heat, transverse ultrasonic vibration, and normal force. The detailed bonding parameters are shown in Table I for the process window optimized by means of pull/shear tests and dimension tests.

In order to accelerate interfacial evolution and ascertain the growth kinetics of Cu-Al IMCs, samples were thermally aged at 200°C for up to 121 days, at 250°C for up to 169 h, and at 300°C for up to 16 h in nitrogen.

After thermal aging, cross-sectional samples were prepared for SEM observation of IMC morphology. Back-scatter electron (BSE) SEM images were taken in order to highlight the presence of different layers (i.e., Al, Cu-Al IMCs, and Cu). The common metallographic procedure was performed to reveal the cross-sectional microstructure: the bonds were wet-ground with grit size 400, 600, 1000, and 2000 sandpaper, followed by polishing with 1.0-μm and 0.25-μm diamond suspensions on silk cloths. SEM observations were performed using a HITACHI S-4700 system. The average thickness of the IMCs was obtained for each sample by measuring the cross-sectional area of the layer over a certain length on the SEM image using an image analyzer.

The microstructure of the Cu-Al bonds both in the as-bonded state and after thermal aging were investigated by cross-sectional TEM combined with EDX. The TEM samples were prepared using FIB with a lift-out technique.[14] Mo lift-out TEM grids were used to avoid x-ray energy overlaps with Cu. TEM analysis was carried out using the JEOL 2100F system at 200 kV. A microprobe beam of

Table I. Optimized bonding parameters

Parameter	Value
Ultrasonic power (DAC)	90
Bonding force (gf)	110
Bonding time (ms)	28
Bonding temperature (°C)	220

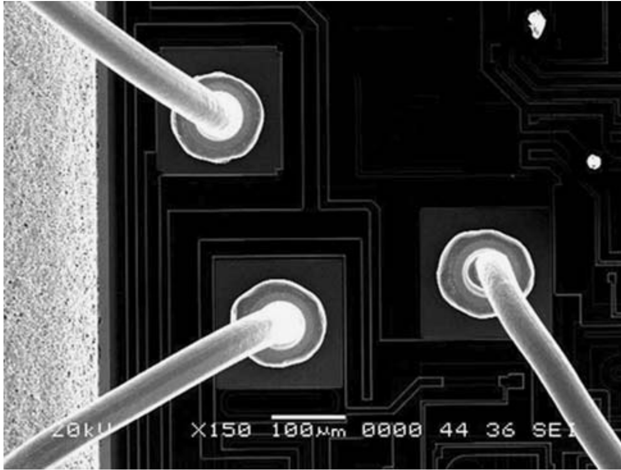

Fig. 1. SEM image of typical copper wire ball bonds formed by thermosonic bonding on aluminum metallization on an IC.

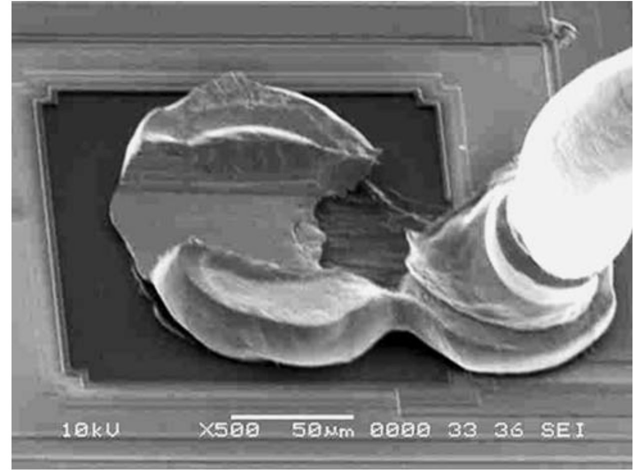

Fig. 2. Failure in mashed copper balls after shear test showing high strength of Cu-Al bonds (average shear force 145 gf).

approximately 1 nm diameter was used for composition analysis with EDX. TEM–SAD was performed to identify the type and structure of Cu-Al IMCs.

RESULTS AND DISCUSSION

Interfacial Morphology of Cu-Al Bonds in As-Bonded State

Cu-Al bonds need to withstand thermal and electrical impacts during device operation, especially at the interface; their initial states and morphology are the key factors for their reliability.[1] Figure 1 shows typical copper-wire ball bonds on aluminum metallization obtained by means of thermosonic bonding with optimized parameters (Table I). The failure in the shear test typically occurs in the mashed copper ball rather than at the interface between the ball and the aluminum metallization pad (Fig. 2); in the pull test it typically occurs as a neck break (Fig. 3), indicating that the Cu-Al bond has high strength.

In order to ascertain the interfacial characteristics of Cu-Al bonds in the as-bonded state, SEM and TEM were employed. A cross-sectional SEM image (Fig. 4) shows no visible IMCs at the interface at such magnification. However, at higher resolution, the bright-field (BF) TEM image (Fig. 5) shows IMCs particles formed between aluminum and copper. Those discontinuous IMC particles are approximately 30 nm thick. Based on our previous work, this very initial phase is $CuAl_2$.[20]

Previous studies of Au-Al bonds based on SEM and TEM observations revealed a 200-nm- to 500-nm-thick Au-Al IMC layer formed at the interface during the thermosonic bonding stage (175°C),[10,11] although the mechanism of formation of Au-Al IMCs within several milliseconds remains unclear. As for Cu-Al bonds, the above morphological analysis showed only approximately 30-nm-thick and discontinuous Cu-Al IMCs at the interface. No voids were observed near the Cu-Al interface; as reported, some nanolevel voids were found inside the Au-Al IMCs for the Au-Al system.[11]

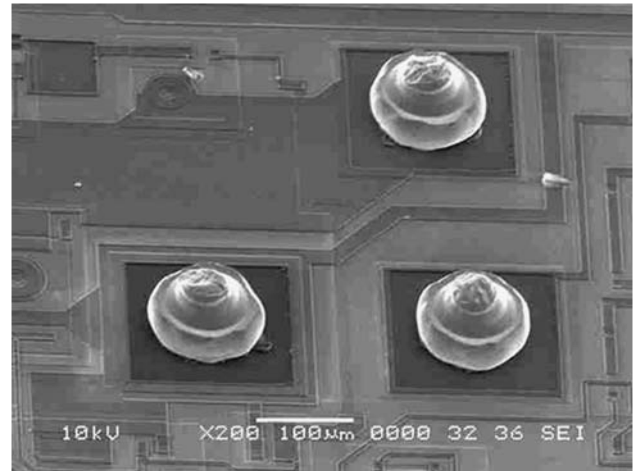

Fig. 3. Failure in necks after pull test, confirming good bondability (average pull force 41 gf).

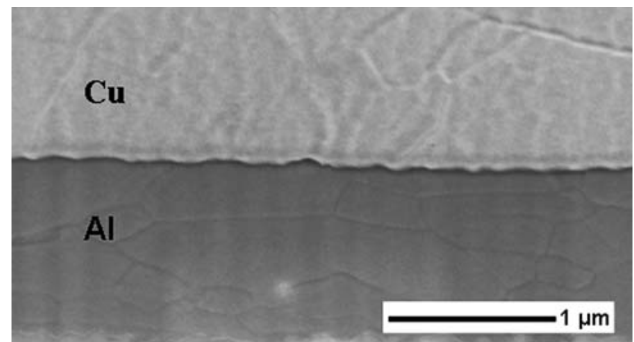

Fig. 4. Cross-sectional SEM image of Cu/Al interface in the as-bonded state.

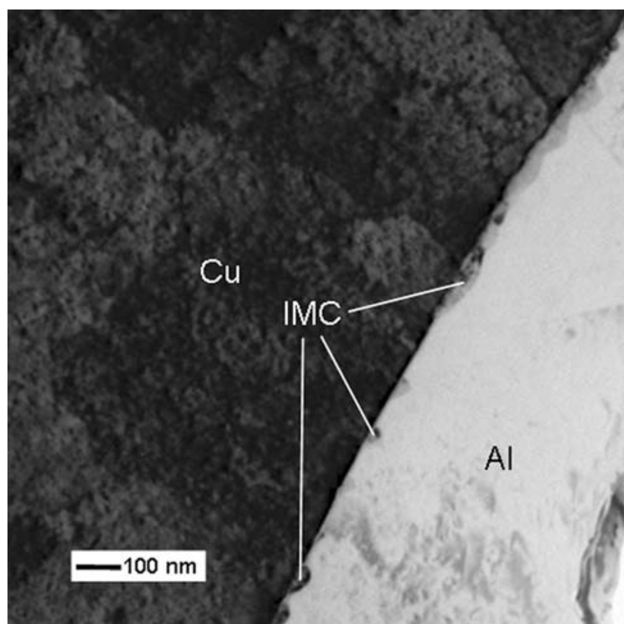

Fig. 5. BF TEM image presenting morphology of interface region of Cu-Al bond.

The real interfacial temperature during the bonding process is expected to account for the bonding mechanism (at least to some extent). The temperature rises up to 320°C based on *in situ* measurements using thin-film thermocouples fabricated by sputtering deposition.[21] Based on the Kuhlmann–Wilsdorf's flash temperature model and the theoretical analysis of frictional energy intensity and real contact area, the calculated magnitude of the temperature rise during the bonding was not more than 321°C.[22] Meanwhile, the morphology of the Cu-Al interface (Figs. 4 and 5) shows no traces of melting, so it can be assumed that thermosonic copper bonding is a solid-state process.

It is well known that the relative motion induced by ultrasonic vibration at the interface plays a very important role in ultrasonic bonding.[1] It can break down surface contaminants and oxides. Thus, pure contact interfaces are partially exposed and contacted; interconnection is the result of IMCs forming during the bonding process due to atomic interdiffusion.

Cu-Al IMCs Growth Kinetics During Thermal Aging

To study the growth behavior of Cu-Al IMCs, thermal aging with different temperatures and durations was performed; the respective cross-sectional BSE SEM images are shown in Figs. 6–8. The basic structures observed at the central interface are the layers of IMCs between the copper wire and aluminum metallization which emerged due to thermal aging. The types of IMCs and their formation sequence will be briefly discussed in the following section. In this section, IMC thickening is observed and quantified based on the total thickness of IMCs at the interface. As a result, the kinetics data obtained are apparent ones based on combined IMC growth behavior.

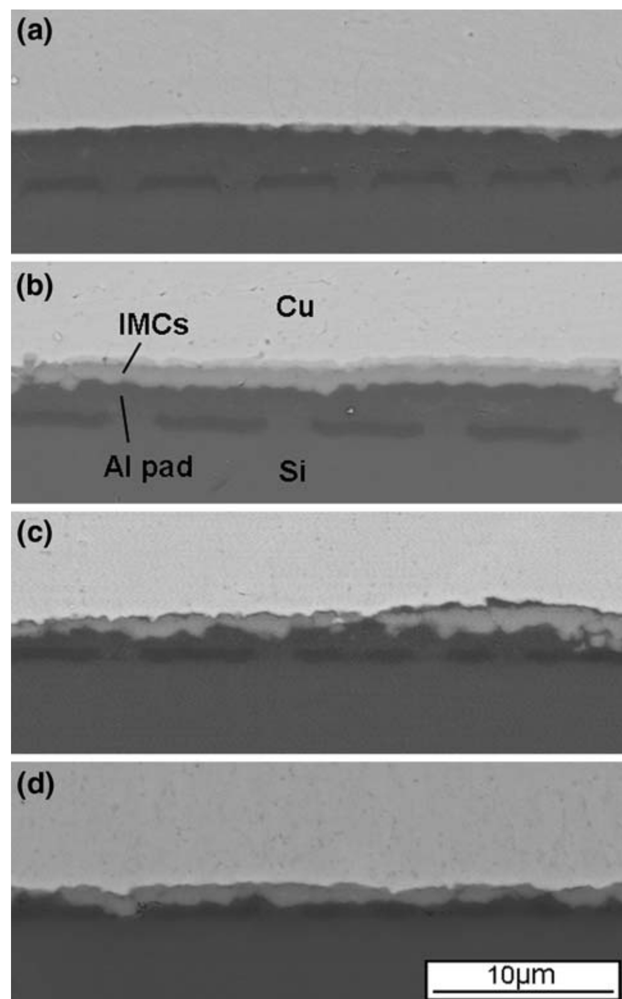

Fig. 6. Cross-sectional BSE SEM of copper ball/Al metallization interfaces after aging at 200°C for: (a) 1 day, very small IMCs formed; (b) 4 days, a layer of IMCs formed; (c) 64 days, thicker IMCs; and (d) 121 days, 1.5-μm-thick IMCs formed.

Figure 6a–d presents cross-sectional BSE SEM images of Cu-Al IMCs formed after thermal aging at 200°C. Very little Cu-Al IMCs were observed at the interface after 1 day of aging (Fig. 6a). Cu-Al IMCs thickened when thermal aging continued but with a low growth rate (Fig. 6b, c). Their thickness reached $\sim$1.5 μm after a long exposure, i.e., 121 days (Fig. 6d).

When aged at 250°C, as shown in Fig. 7a–d, IMCs grew much faster than at 200°C. Evidently, the layers of IMCs have formed after 25 h of aging. Al metallization was consumed due to its reaction with copper, and it completely disappeared after 169 h.

The morphological changes that occurred during thermal aging at 300°C are shown in Fig. 8a–d. The IMCs became obvious at the Cu/Al interface even after only 1 h of aging, and IMCs increased rapidly

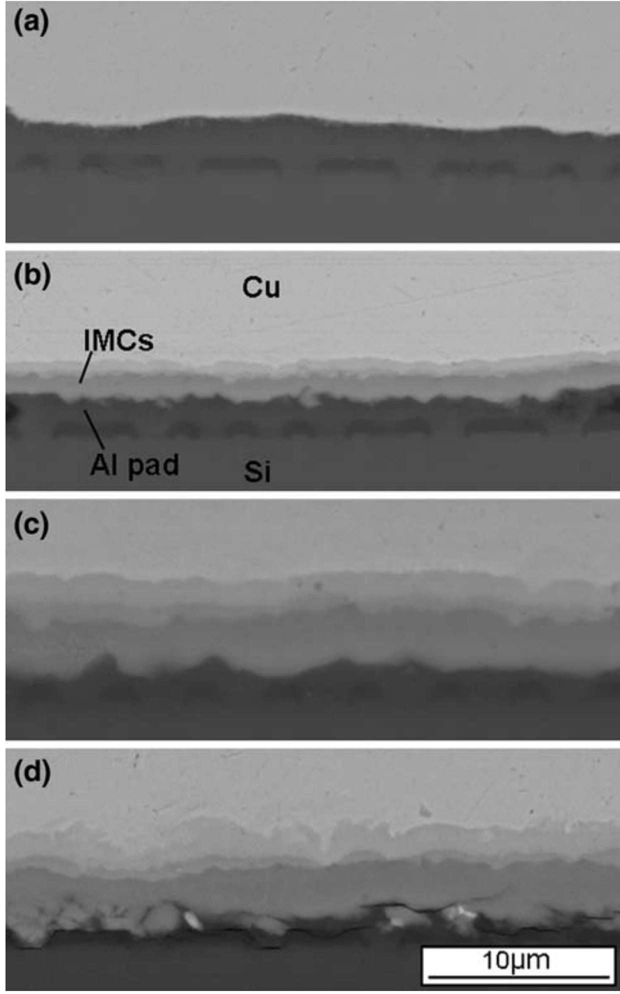

Fig. 7. Cross-sectional BSE SEM images of copper ball/Al metallization interfaces after aging at 250°C for: (a) 1 h; (b) 25 h; (c) 100 h; and (d) 169 h. Al metallization thinned with increasing time and disappeared after 169 h.

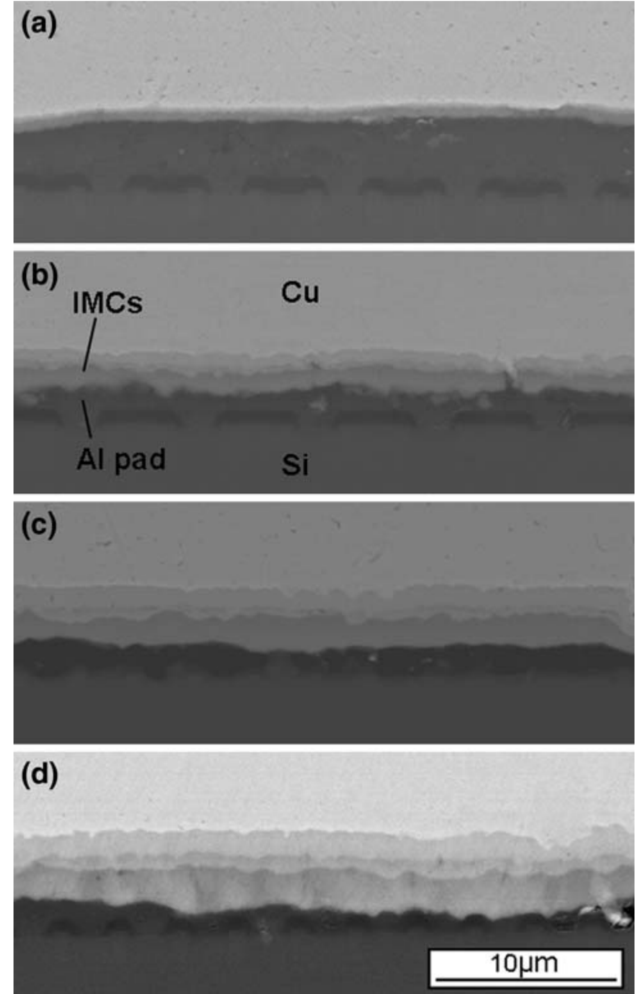

Fig. 8. Cross-sectional BSE SEM images of Cu-Al samples aged at 300°C for: (a) 1 h; (b) 4 h; (c) 9 h; and (d) 16 h.

with thermal treatment. Aluminum metallization was almost consumed after only 16 h.

In a solid-state reaction analysis, the thickness x of IMCs at aging time t was estimated using the following equation[15]:

$$x - x_1 = (Kt)^{1/n}, \quad (1)$$

where K is the growth rate constant, x_1 is a constant related to the initial IMC thickness, and n is the time index.

The magnitude of the growth rate constant of IMCs changes for different types of Cu-Al IMCs; it also depends on the neighboring phases, which supply additional Cu and/or Al for continued compound formation. However, it is extremely difficult to measure the thickness of each individual IMC layer, as they intertwine with each other. Therefore, a combined growth rate constant and activation energy for all potential Cu-Al IMCs formed in bonds were introduced. Figure 9 shows the thickness of Cu-Al IMCs for samples aged for various times at 200°C, 250°C, and 300°C. In general, the solid-state growth of IMCs can follow linear or parabolic growth kinetics. Linear growth implies that the growth rate is limited by the reaction rate at growth sites. In contrast, parabolic growth implies that the growth is controlled by diffusion. It is obvious from Fig. 9 that the growth of IMCs follows a parabolic law (n = 2), suggesting that the Cu-Al IMCs growth during thermal aging is a diffusion-controlled process. Cu-Al IMCs grew faster at the earlier stage of aging, and the process was more sensitive to the aging temperature than to the aging time. The growth rate constants for Cu-Al IMCs (Table II) were calculated from the fitted parabolas in Fig. 9.

According to the classic kinetic theory, the value of K is characterized by the temperature and activation energy, and it can be given by the Arrhenius equation[17,23,24]:

$$K = K_0 \exp\left(-\frac{Q}{RT}\right), \quad (2)$$

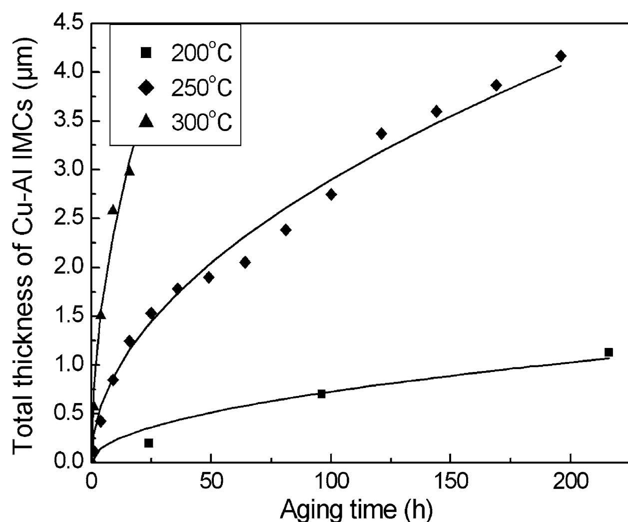

Fig. 9. Cu-Al IMC growth in Cu-Al bonds under different thermal aging times and temperatures.

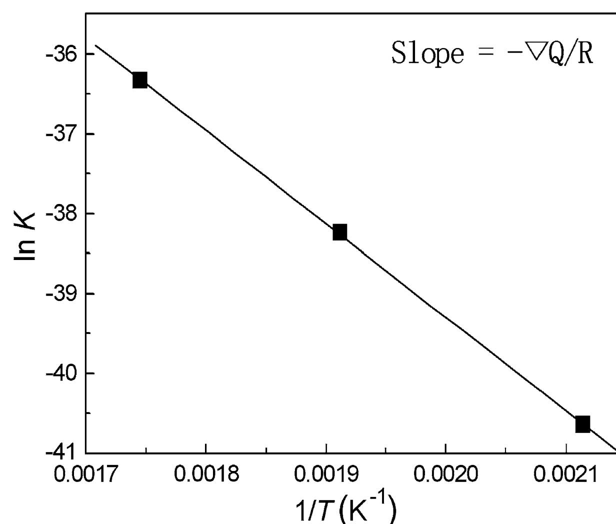

Fig. 10. ln K versus $1/T$ dependence.

Table II. Growth rate constants for IMCs in Cu-Al bonds at different temperatures

T, Temperature (°C)	K, Growth Rate Constants for Cu-Al IMCs (m^2/s)
200	2.27×10^{-18}
250	2.46×10^{-17}
300	1.67×10^{-16}

where K_0 is a prefactor, Q is the activation energy for intermetallic growth, R is the molar gas constant, and T is absolute temperature.

An Arrhenius plot, as shown in Fig. 10, is obtained from the data in Table II. The activation energy, Q, can be calculated from the slope of a curve of ln K versus $1/T$. The obtained activation energy was 1.01 eV, which was different from the reported activation energy, 1.14 eV to 1.43 eV, obtained for the bulk Cu/Al diffusion couples.[25,26]

A lower activation energy is generally considered an indication of the formation of IMCs by short-circuit diffusion via structural defects such as grain boundaries and dislocations. Actually, the atomic diffusion of Cu and Al through the IMCs is the main defining process for the IMCs growth during thermal aging. During diffusion, one atom moves into an empty lattice position (vacancy), and another atom moves into the empty position of the first. Therefore, the diffusion rate of one metal into another is dependent on the number of defects (e.g., vacancies, dislocations, and grain boundaries) in the crystal lattice. The more defects it has, the faster the diffusion processes. The thermosonic bonding process results in numerous lattice defects for Cu-Al bonds due to large plastic deformations and high stresses, thus, interdiffusion in thermosonic bonds is more rapid than in bulk Cu/Al couples; this explains the lower activation energy of Cu-Al IMCs in thermosonic Cu-Al bonds. As a consequence, poorly bonded bonds would fail more rapidly as IMCs grow more quickly.

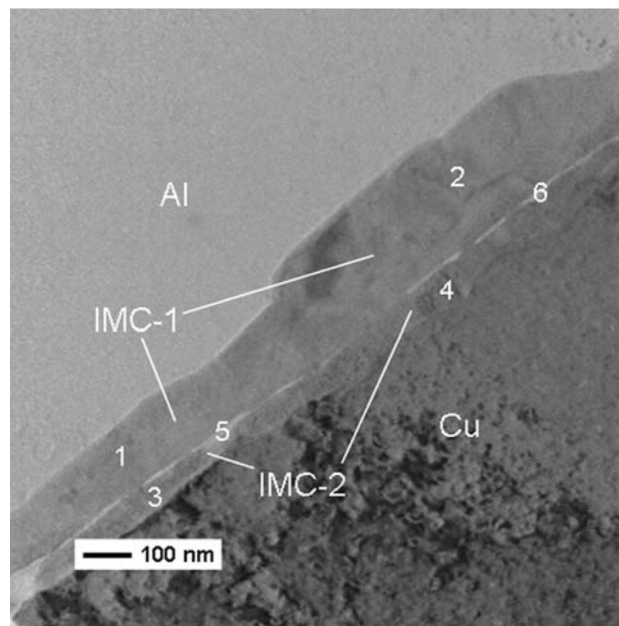

Fig. 11. TEM image presenting two layers of IMCs in Cu-Al bond after thermal aging at 250°C for 1 h.

Identification of Cu-Al IMCs

Figure 11 presents a BF TEM image of the interface region of a Cu-Al bond after thermal aging for 1 h at 250°C. Two layers of IMCs are clearly observed between copper and aluminum.

STEM–EDX was conducted to identify these IMC layers. The results of EDX given in Table III from

Table III. STEM–EDX results of regions 1–6 in Fig. 11

Regions	O K (at.%)	Al K (at.%)	Cu K (at.%)
1	10.8	46.2	43.0
2	9.9	46.7	43.4
3	11.1	26.5	62.4
4	12.1	27.2	60.6
5	48.9	31.0	20.2
6	40.5	37.2	22.3

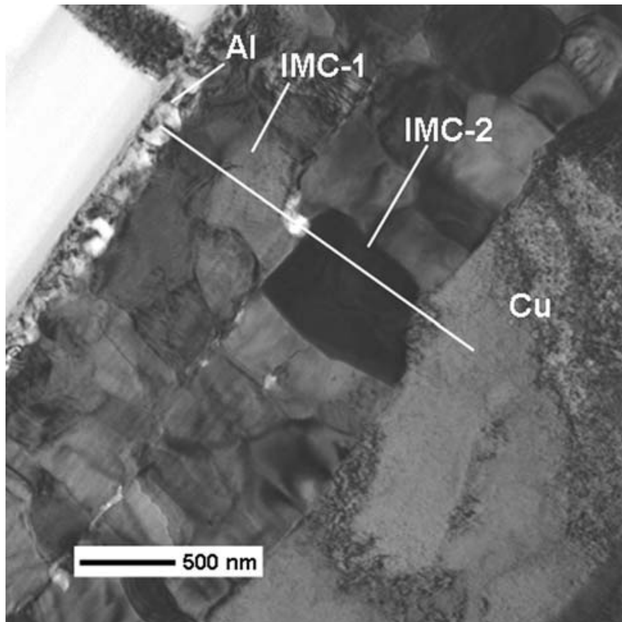

Fig. 12. TEM image of a Cu-Al bond after thermal aging at 250°C for 100 h.

regions 1 and 2 of the IMC-1 layer indicate that the ratio of Cu to Al was close to 1:1; however, an approximate 9:4 Cu-to-Al ratio was found in regions 3 and 4 of the IMC-2 layer. Therefore, the two types of IMCs (CuAl and Cu_9Al_4) existed in the layers of IMC-1 and IMC-2, respectively. It was also found with EDX that oxygen is relatively rich at the interface between the two IMCs (approximately 40 at.% to 50 at.%) in comparison with inside the IMCs (approximately 10 at.%).

A TEM image of a sample after thermal aging for 100 h at 250°C is shown in Fig. 12. Two thicker layers of IMCs existed between the copper and aluminum.

Line-scanning TEM–EDX analysis was conducted across those two layers of Cu-Al IMCs, and the results are shown in Fig. 13. As there are no changes in the composition between the two layers of IMCs, it indicates that there could be only one type of IMC between the Cu and Al. The decrease of intensity of all elements at the interface between

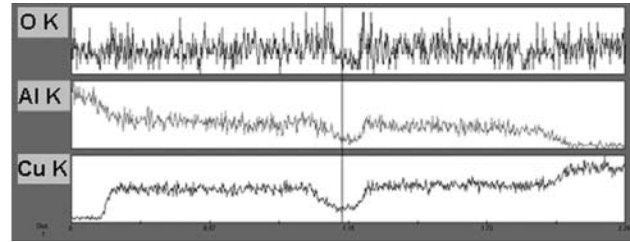

Fig. 13. Results of line-scanning TEM–EDX across two layers of IMCs in Fig. 12.

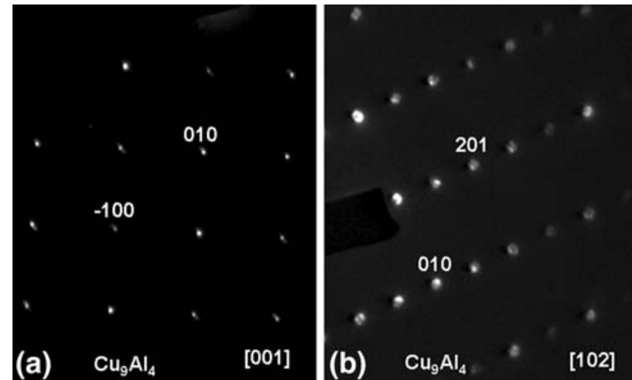

Fig. 14. SAD patterns of (a) IMC-1 and (b) IMC-2 in Fig. 12.

the two layers of IMCs indicates the presence of voids.

Due to the inability to identify the crystallographic structure by means of TEM–EDX analysis, further investigation was carried out by TEM–SAD, with two diffraction patterns of Cu-Al IMCs for the sample aged at 250°C for 100 h presented in Fig. 14a and b. Cu_9Al_4 (p-43m, a = 0.870 nm) was identified as the phase for both IMC layers. For the sample aged at 250°C for 1 h, SAD results showed that both IMCs are polycrystalline, although further identification is still ongoing. However, it should be noted that STEM–EDX suggested that two layers of IMCs might be CuAl and Cu_9Al_4, respectively. Previous work investigating interdiffusion in bulk copper–aluminum couples detected all five equilibrium phases by microprobe analysis,[15] and observed $CuAl_2$, CuAl and Cu_9Al_4 in thin-film copper–aluminum couples.[16,17]

The presence of specific intermetallic phases can depend on the relative amounts of metals present in the initial composition. Bulk copper–aluminum couples and thin-film couples with varying relative amounts of metals could produce different compounds. Consequently, for copper bonds on aluminum metallization, the amount of copper is much higher than that of aluminum, producing copper-rich IMCs, i.e., Cu_9Al_4. However, it is possible that other phases are initially formed at the early stage of diffusion but are dissolved or transferred to another phase when one of the materials is consumed in the diffusion process or reaction. We believe that,

in our Cu-Al bonded samples, $CuAl_2$ was the initial phase formed at scattered sites of the interface. Upon aging treatment, CuAl phase formed as a result of more Cu diffusion through the interface. At the same time Cu_9Al_4 started to form adjacent to the Cu side, probably due to the relative ease of its nucleation. Once the thin Al layer was fully consumed, the CuAl phase transformed into Cu_9Al_4. This is evidenced by the coexistence of CuAl and Cu_9Al_4 in the sample aged at 250°C for 1 h (Fig. 11). However, CuAl finally transformed into Cu_9Al_4 when aluminum was consumed after 100 h (Fig. 12).

CONCLUSIONS

TEM studies of interfacial features of Cu-Al bonds in the as-bonded state showed that approximately 30-nm-thick and discontinuous Cu-Al IMCs were formed. Thus, thermosonic copper wire bonding on aluminum metallization is proposed to be metallurgical and chemical bonding.

The evolution of Cu-Al IMCs was observed as a result of thermal aging of Cu-Al bonds. The growth of IMCs was found to follow a parabolic law, indicating that it was controlled by the diffusion mechanism. The combined activation energy calculated for the growth of Cu-Al IMCs was 1.01 eV, which is smaller than reported values obtained for bulk Cu/Al diffusion couples. An explanation was given based on the fact that more defects were generated in the thermosonic bonding process, leading to faster interdiffusion in Cu-Al bonds.

Two types of Cu-Al IMCs (CuAl and Cu_9Al_4) were present after 1 h of aging at 250°C. However, Cu_9Al_4 was identified as the only IMC after 100 h of aging at 250°C. Analysis showed that the relative short supply of aluminum could be the cause of formation of copper-rich IMCs, i.e., Cu_9Al_4.

ACKNOWLEDGEMENTS

This paper is an output of the PMI2 Project funded by the UK Department for Innovation, Universities, and Skills (DIUS) for the benefit of the Singapore Higher Education Sector and the UK Higher Education Sector. Authors would also like to acknowledge Dr. Geoff West, Mr. John Bates, and Mr. Honghui Wang for their assistance with experiments.

REFERENCES

1. G.G. Harman, *Wire Bonding in Microelectronics, Materials, Processes, Reliability, and Yield*, 2nd ed. (New York: McGraw-Hill, 1997).
2. E. Philofsky, *Solid State Electron.* 13, 1391 (1970).
3. G.Y. Jang, J.G. Duh, H. Takahashi, and D. Su, *J. Electron. Mater.* 35, 323 (2006).
4. H. Ji, M. Li, C. Wang, and H.S. Bang, *Mater. Sci. Eng. A* 447, 111 (2007).
5. H.S. Chang, J.X. Pon, K.C. Hsieh, and C.C. Chen, *J. Electron. Mater.* 30, 1171 (2001).
6. S. Murali, *J. Alloy Compd.* 426, 200 (2006).
7. S. Murali, N. Srikanth, and C.J. Vath, *Mater. Lett.* 58, 3096 (2004).
8. N. Srikanth, S. Murali, Y.M. Wong, and C.J. Vath, *Thin Solid Films* 462–463, 339 (2004).
9. S. Murali, N. Srikanth, Y.M. Wong, and C.J. Vath, *J. Mater. Sci.* 42, 615 (2007).
10. C.D. Breach and F. Wulff, *Microelectron. Reliab.* 44, 973 (2004).
11. A. Karpel, G. Gur, Z. Atzmon, and W. Kaplan, *J. Mater. Sci.* 42, 2334 (2007).
12. P. Ratchev, S. Stoukatch, and B. Swinnen, *Microelectron. Reliab.* 46, 1315 (2006).
13. S. Murali, N. Srikanth, and C.J. Vath, *Mater. Res. Bull.* 38, 637 (2003).
14. H.J. Kim, J.Y. Lee, K.W. Paik, K.W. Koh, J.H. Won, S.Y. Choe, J. Lee, J.T. Moon, and Y.J. Park, *IEEE Trans. Compon. Packag. Technol.* 26, 367 (2003).
15. Y. Funamizu and K. Watanabe, *Trans. Jpn. Inst. Met.* 12, 147 (1971).
16. Y. Tamou, J. Li, S.W. Russell, and J.W. Mayer, *Nucl. Instrum. Methods B* 64, 130 (1992).
17. K. Rajan and E.R. Wallach, *J. Cryst. Growth* 49, 297 (1980).
18. J.P. Lokker, A.J. Böttger, W.G. Sloof, F.D. Tichelaar, G.C.A.M. Janssen, and S. Radelaar, *Acta Mater.* 49, 1339 (2001).
19. M. Koberna and J. Fiala, *Mater. Sci. Eng. A* 159, 231 (1992).
20. H. Xu, C. Liu, V.V. Silberschmidt, S.S. Pramana, T.J. White, and Z. Chen, *Scripta Mater.* 61, 165 (2009).
21. J.R. Ho, C.C. Chen, and C.H. Wang, *Sens. Actuators A* 111, 188 (2004).
22. Y.R. Jeng and J.H. Horng, *J. Tribol.* 123, 725 (2001).
23. Y. Tanaka, M. Kajihara, and Y. Watanabe, *Mater. Sci. Eng. A* 445–446, 355 (2007).
24. M. Kajihara, *Mater. Sci. Eng. A* 403, 234 (2005).
25. W.B. Lee, K.S. Bang, and S.B. Jung, *J. Alloy Compd.* 390, 212 (2005).
26. M. Braunovic and N. Alexandrov, *IEEE Trans. Compon. Packag. Manuf. Technol.* 17, 78 (1994).